The Journal of Immunology

Activation of Adenosine 2A Receptors Attenuates Allograft Rejection and Alloantigen Recognition

Charles P. Sevigny, Li Li, Alaa S. Awad, Liping Huang, Marcia McDuffie, Joel Linden, Peter I. Lobo and Mark D. Okusa

J Immunol 2007; 178:4240-4249; ;
doi: 10.4049/jimmunol.178.7.4240
http://www.jimmunol.org/content/178/7/4240

The Journal of Immunology is published twice each month by
The American Association of Immunologists, Inc.,
1451 Rockville Pike, Suite 650, Rockville, MD 20852

Print ISSN: 0022-1767 Online ISSN: 1550-6606.

Activation of Adenosine 2A Receptors Attenuates Allograft Rejection and Alloantigen Recognition[1]

Charles P. Sevigny,[2]* Li Li,[2]* Alaa S. Awad,* Liping Huang,* Marcia McDuffie,† Joel Linden,*‡§ Peter I. Lobo,* and Mark D. Okusa[3]*‡§

The current studies investigated the in vitro and in vivo effect of adenosine 2A receptor ($A_{2A}R$) agonists to attenuate allogenic immune activation. We performed MLRs with spleen T lymphocytes and APCs isolated from wild-type and $A_{2A}R$ knockout mice of both C57BL/6 and BALB/c background strains. Two-way MLR-stimulated T cell proliferation was reduced by ATL313, a selective $A_{2A}R$ agonist in a dose-responsive manner (~70%; 10 nM), an effect reversed by the $A_{2A}R$ antagonist ZM241385 (100 nM). By one-way MLRs, we observed that ATL313's inhibitory effect was due to effects on both T cells and APCs. ATL313 suppressed the activation markers CD25 and CD40L and the release of inflammatory cytokines IFN-γ, RANTES, IL-12P_{70}, and IL-2. ATL313 also increased negative costimulatory molecules programmed death-1 and CTLA-4 expressed on T cells. In lymphocytes activated with anti-CD3e mAb, ATL313 inhibited the phosphorylation of Zap70, an effect that was reversed by the protein kinase A inhibitor H-89. In skin transplants, allograft survival was enhanced with ATL313, an effect blocked by ZM241385. These results indicate that $A_{2A}R$ agonists attenuate allogenic recognition by action on both T lymphocytes and APCs in vitro and delayed acute rejection in vivo. We conclude that $A_{2A}R$ agonists may represent a new class of compounds for induction therapy in organ transplantation. *The Journal of Immunology,* **2007, 178: 4240–4249.**

Innate and adaptive immunity critically impacts acute and chronic allograft rejection as well as ischemia-reperfusion injury (IRI),[4] and the ability to attenuate these effects could consistently enhance long-term allograft survival. T cells play a critical role in the pathogenesis of acute and chronic allograft rejection (1). Activation of T cells requires specific signaling by the interaction between the TCR and Ag presented by APCs and is also regulated by positive and negative costimulatory signals. B7 family ligands and receptors play an important role in controlling the activation and proliferation of T cells. Interaction of B7-1 (CD80) and B7-2 (CD86) expressed on APCs with CD28 expressed on T cells promotes T cell expansion and cytokine secretion (2). In contrast, interaction of B7-1 and B7-2 with CTLA-4 expressed on T cells, which is up-regulated after T cell activation, suppresses T cell activation (3, 4). Programmed death (PD)-1 expressed on T cells is another inhibitory molecule regulated by IFN-γ, which binds to the APC ligands PD-L1 (B7-H1) and PD-L2 (B7-DC). PD-L1 shares 20–38% aa identity with other B7 family members (B7-1 and B7-2) expressed on APCs and nonlymphoid tissues. Upon T cell activation, up-regulation of PD-1 expression also contributes to T cell homeostasis (5). Thus, the negative costimulatory pathways CTLA-4:B7 and PD-1:PD-L down-regulate T cell-mediated alloimmunity, and studies in animals would support the concept that PD-1 and CTLA-4 can induce transplantation tolerance.

Adenosine 2A receptors ($A_{2A}Rs$) are a subtype of the G protein-coupled receptor family of adenosine receptors, which also includes A_1R, $A_{2B}R$, and A_3R (6, 7), and they have tissue protective properties (8). Systemically administered $A_{2A}R$ agonists have been shown to reduce tissue injury associated with ischemia-reperfusion (9–12). Through a series of studies, we demonstrated that the protective effect of $A_{2A}R$ agonists was mediated through bone marrow-derived leukocytes (13). Furthermore, additional studies indicate that $A_{2A}R$ agonists reduce kidney IRI through activation of $A_{2A}Rs$ expressed on $CD4^+$ cells (14). $A_{2A}R$ agonists, including ATL313, attenuate IFN-γ and limit anti-CD3e mAb-induced T cell activation (15). Delayed graft function is a form of IRI that is thought to increase the immunogenicity of the transplanted allograft (8) in part due to an increase in MHC class I and II expression leading to episodes of acute rejection and chronic graft loss. These findings suggest that $A_{2A}Rs$ may be uniquely suited to block T cell activation associated with IRI and delayed graft function. Moreover, given the diverse effects of $A_{2A}R$ activation on T cell function, we considered the possibility that $A_{2A}R$ activation attenuates allogenic recognition, thus rendering agonists of $A_{2A}Rs$ useful in attenuating rejection in transplantation.

In the current study, we sought to determine the effect of $A_{2A}R$ agonists in vitro on alloantigen-induced T cell activation and proliferation as well as the effect of costimulatory molecules. We studied the effect of $A_{2A}R$ activation on the MLR, an assay in which the lymphocytes from two separate mouse strains are combined and cultured in vitro to initiate an alloimmune response. An advantage of this approach is that T cell activation occurs under physiological conditions that involve TCR activation and Ag presented by dendritic cells (DCs) and that are regulated by positive

*Department of Medicine, †Department of Microbiology, ‡Cardiovascular Research Center, and §Carter Immunology Center University of Virginia, Charlottesville, VA 22908

Received for publication January 30, 2006. Accepted for publication January 10, 2007.

The costs of publication of this article were defrayed in part by the payment of page charges. This article must therefore be hereby marked *advertisement* in accordance with 18 U.S.C. Section 1734 solely to indicate this fact.

[1] This work was supported by National Institutes of Health Grants DK56223, DK62324, DK58413, and HL37942.

[2] C.P.S. and L.L. participated equally in this study.

[3] Address correspondence and reprint requests to Dr. Mark D. Okusa, Division of Nephrology, Box 800133, University of Virginia Health System, Charlottesville, VA 22908. E-mail address: mdo7y@virginia.edu

[4] Abbreviations used in this paper: IRI, ischemia-reperfusion injury; $A_{2A}R$, adenosine 2A receptor; DC, dendritic cell; KO, knockout; MCF, mean channel fluorescence; PD, programmed death; PKA, protein kinase A; WT, wild type.

and negative costimulatory molecules. In vitro studies demonstrate that, in response to T cell activation by alloantigens, $A_{2A}R$ agonists attenuate T cell activation and decrease secretion of proinflammatory cytokines through direct and independent effects on both T cells and APCs. Importantly, the $A_{2A}R$ agonist increased expression of negative costimulatory molecules PD-1 and CTLA-4 that are involved in peripheral tolerance. Lastly, we demonstrated that the in vitro inhibitory effects of $A_{2A}R$ agonists on alloantigen-induced immune response likely contribute to the attenuation of tissue rejection following skin transplantation. These results suggest that $A_{2A}R$ activation is a unique and potent strategy in attenuating IRI and delaying allograft rejection following organ transplantation.

Materials and Methods

Animals

All animals were handled and procedures were performed in adherence to the National Institutes of Health Guide for the Care and Use of Laboratory Animals and in accordance with the University of Virginia Animal Care and Use Committee protocols. C57BL/6 (B6) and BALB/c mice were purchased from Charles River Laboratories. The source and derivation of congenic $A_{2A}R$ knockout (KO) mice was described previously (13, 16). To generate Adora2a^{null} (A_{2A}RKO) mice congenic to BALB/c (17–19), a mapping panel of 55 microsatellite loci informative for a (C57BL/6J × BALB/cByJ) cross was identified with coverage for every chromosome, except X and Y, at a density of <30 cM. The mapping panel is available on request (mjm7e@virginia.edu). A single founder male was mated to BALB/cByJ female mice. (BALB/c × B6.129-Adora2a^{tm1jfc})F_1 males carrying the Adora2a mutation were then mated to BALB/cByJ females in two successive generations of backcrossing with breeders selected for maximal BALB/cByJ homozygosity. The BALB/cByJ Y chromosome was introduced by crossing BALB/cByJ males to genotypically selected F1N3 females carrying the Adora2a mutation in the final backcross generation before initiation of inbreeding with F1N4 mice of both sexes. Residual B6 or 129 alleles in the congenic line were detected only on mouse chromosome 10 between Adora2a and D10Mit35 (74.77–121.60 Mb, respectively; NCBIm36).

Harvesting of mouse splenocytes

Spleens were extracted from B6 and BALB/c mice and disrupted under sterile conditions in PBS through 40-μm BD Falcon cell strainers (Fisher Scientific). Leukocytes were then isolated via density gradient centrifugation using Histopaque 1083 (Sigma-Aldrich) and washed in RPMI 1640 supplemented with 10% heat-inactivated FBS (Invitrogen Life Technologies) and 1% antibiotic/antimitotic solution (Invitrogen Life Technologies). Cells were resuspended (1×10^6 cells/ml) in the culture medium in the presence of adenosine deaminase (1 U/ml; Roche Diagnostics).

Activation of lymphocytes by alloantigens by MLRs

In two-way MLR assays, 2×10^5 leukocytes from B6 mice in 0.1 ml were cocultured with an equal number of leukocytes from BALB/c mice using 96-well flat-bottom tissue culture-treated plates. Appropriate compounds were administered at the initiation of the two-way MLR assay. All compounds were diluted in 10 μl of medium before being added to the appropriate wells, and cells were allowed to incubate at 37°C in the presence of 5% CO_2. As controls, we added vehicle without compound to cell cultures. Second, in two-way MLR assays, cells obtained from each murine strain were cultured alone, i.e., without mixing, so as to calculate the added effect obtained with cocultures.

For one-way MLR studies, cell cultures were prepared as described previously (20). Stimulator cells were prepared from spleens of wild-type (WT) (B6 background) or A_{2A}KO (B6 background) mice. Spleens were cut into small pieces and digested with 1 mg/ml collagenase type IA (Sigma-Aldrich) for 10 min at 37°C, which can increase the yield of APCs. Single-cell suspension was treated with mitomycin C (50 μg/ml; Sigma-Aldrich) for 20 min at room temperature and then washed twice with RPMI 1640. Responder spleen T cells from spleens of WT (BALB/c background) or A_{2A}KO (BALB/c background) mice were harvested by negative isolation using magnetic beads, according to the manufacturer's protocol (Dynal T Cell Negative Isolation kit; Invitrogen Life Technologies). The purity of the CD3 T cells was measured by FACS (BD Biosciences), and T cells with >98% purity were used in this study. Responder (2×10^5) and stimulator (4×10^5) cells were added to round-bottom 96-well plates to a final volume of 200 μl of RPMI 1640 with 10% FCS/1% antibiotic/antiamitotic solution and in the presence of adenosine deaminase (1 U/ml; Roche Diagnostics). Each experiment was performed in triplicate.

Vehicle or 4-[3-[6-amino-9-(5-cyclopropylcarbamoyl-3,4-dihydroxy-tetrahydro-furan-2-yl)-9*H*-purin-2-yl]-prop-2-ynyl]-piperidine-1-carboxylic acid methyl ester (ATL313) was used in two-way (0.01–100 nM) and one-way (10 nM) MLRs. 4-(2-[7-Amino-2-[2-furyl][1,2,4]triazolo[2,3-*a*][1,3,5]triazin-5-yl-amino]ethyl)phenol (ZM241385) (100 nM) was used to determine specificity of ATL313 for the $A_{2A}R$.

Activation of lymphocytes by anti-CD3e

In these studies, leukocytes were activated with anti-CD3e mAb. Functional grade hamster anti-mouse CD3e mAb (clone 145-2C11; eBioscience) was used in an insoluble form (by precoating tissue culture-treated plates) or in soluble form. Plates were coated by covering wells with Ab in PBS (2 μg/ml) for 4 h at 37°C, then rinsed twice with PBS before adding cells. Soluble Ab was used at different concentrations at the initiation of the culture. Controls were the same as the two-way MLR assay.

Proliferation assays

Lymphocytes activated in an MLR or by anti-CD3e mAb were allowed to incubate up to 3 days before harvesting. [^{3}H]Thymidine (0.5 μCi/well; MP Biomedicals) was added 18–24 h before harvesting (Skatron Instruments) using Type A filter mats (PerkinElmer Life and Analytical Sciences) and beta plate scintillation mixture (PerkinElmer). Disintegrations per minute were determined using a liquid scintillation counter (1205 Betaplate; PerkinElmer).

Multiplex bead array for quantitating cytokines

Multiplex bead array was performed on supernatants obtained on day 3 of culture. Microbead labeling was performed using the Bio-Plex multiplex cytokine assay kit (Bio-Rad) in accordance with manufacturer's protocol, and cytokine levels were analyzed on the Bio-Plex system (Bio-Rad).

ELISA for quantitating IFN-γ

ELISA was performed on supernatants obtained on day 3 of culture. The ELISA for IFN-γ (IFN-γ Ready, Set, Go! ELISA kit; eBioscience) was performed according to manufacturer's protocol and analyzed on a Model 680 microplate reader (Bio-Rad).

Multiprobe RNase protection assay

Total RNA was prepared using RNAzol B (Leedo Medical Laboratories) and analyzed by 1.5% agarose gel electrophoresis to assess the integrity of RNA before solution hybridization. Cytokine mRNA expression was assessed by BD RiboQuant Multiprobe RNase protection system (BD Pharmingen), according to the manufacturer's protocol. In brief, mRNA-specific RNA probes were labeled with ^{32}[P]UTP using multiprobe template sets (mCK3b; BD Pharmingen) for cytokine genes. Total cellular RNA was subjected to solution hybridization with each probe set. Hybridization was performed at 56°C before RNase treatment. Following RNase treatment, protected fragments were separated by gel electrophoresis on 5% polyacrylamide gels and exposed to Kodak X-Omat AR film at −70°C with a single intensifying screen. Band densities were quantitated using the Personal Densitometry SI (GE Healthcare), and data were analyzed by ImageQuant 5.2 (GE Healthcare).

Flow cytometry

All flow cytometry was performed on a BD FACSCalibur flow cytometer (BD Biosciences), and data were analyzed with FlowJo software 4.2 (Tree Star). Most of the Abs were purchased from eBioscience.

Apoptosis/Necrosis

An Annexin V^{FITC} apoptosis detection kit (BD Pharmingen) was used to analyze MLR-activated lymphocytes after 72 h of culture with the control vehicle or ATL313 (10 nM) with or without ZM241385 (100 nM). Cultured cells (1×10^6 cells/ml) were washed with cold PBS and resuspended in annexin V binding buffer. The cell suspension (100 μl) was mixed with annexin V (5 μl) and propidium iodide (5 μl) in a 5-ml culture tube and incubated for 15 min in the dark at room temperature. A total of 400 μl of binding buffer was added to each sample before analysis by flow cytometry.

CD4/CD25 and CD4/CD40L

Three-day two-way MLR-activated cells were washed with 1% BSA/PBS and labeled with anti-mouse CD4-allophycocyanin (GK1.5; 4 μg/ml) and

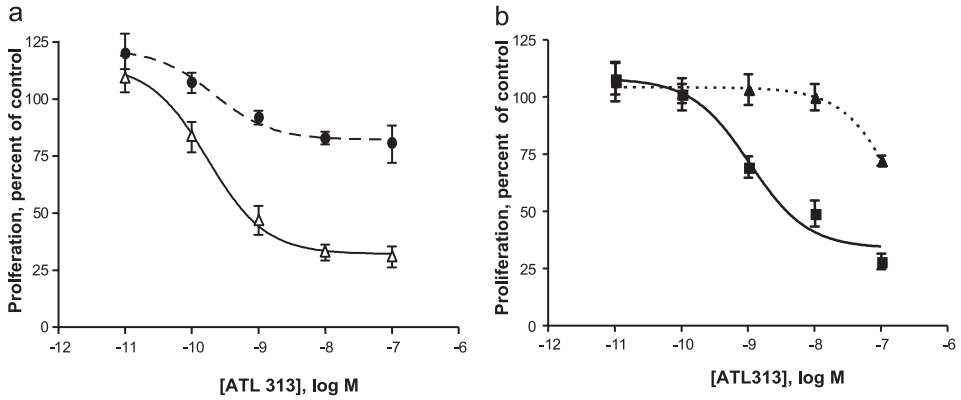

FIGURE 1. ATL313 activates A_{2A}Rs and reduces lymphocyte proliferation. *a*, The effect of ATL313 on the proliferative response in two-way MLRs was examined in the absence (solid line, $n = 8$) and presence (dashed line, $n = 6$) of ZM241385 (100 nm). Values are means ± SEM and are calculated as percent increase in proliferation of cells compared with control vehicle-treated cells. Under vehicle conditions, [^{3}H]thymidine incorporation in two-way MLRs, a measure of cell proliferation, ranged from 10,000 to 20,000 dpm/well. *b*, Reduction of proliferation by ATL313 in anti-CD3e mAb-activated lymphocytes. The effects of ATL313 on lymphocyte proliferation were examined after 24 h of activation by plate-bound anti-CD3e mAb in both WT (solid line, $n = 4$) and A_{2A}RKO (dotted line, $n = 4$) B6 background splenocytes. Values depict mean normalized percentages between control anti-CD3e mAb-induced proliferation (vehicle-treated) and nonactivated lymphocytes (0%) ± SEM. Activated lymphocytes under vehicle treatment demonstrated a range of ~20,000–30,000 dpm/well.

either anti-mouse CD25-PE (PC61.5; 4 μg/ml) or anti-mouse CD40L-PE (MR1; 4 μg/ml) in 25 μl of 0.2% BSA/PBS after blocking FcRs by CD16/32 (2.4G2; eBioscience) for 30 min on ice. Isotype controls were also performed. Samples were washed with 0.2% BSA/PBS and 2 μg/ml 7-aminoactinomycin D (Invitrogen Life Technologies) before analysis by flow cytometry.

CD4/P-Zap70

Spleen cells were isolated from B6 mice as described above, then incubated with soluble anti-CD3e mAb (145-2C11; 10 μg/ml) to stimulate lymphocytes (1×10^6) for 5 min with or without ATL313 (10 nM) or with or without ZM241385 (100 nM). Due to the short reaction time in the presence of soluble anti-CD3e mAb, the cells were pretreated with the compounds for 30 min before stimulation with the Ab. Adding 4 volumes of cold PBS terminated the reaction. Cells were collected by centrifugation and then fixed with 2% formaldehyde for 10 min at room temperature, centrifuged again, and rinsed once with PBS. The supernatant was discarded, and the tubes were chilled on ice for 1 min. Ice-cold methanol (90%) was added slowly during gentle vortexing before incubating the suspension for 30 min on ice. Cells were centrifuged and resuspended in 0.5% BSA/PBS and anti-mouse CD16/32 (2.4G2; 10 μg/ml) for 10 min at room temperature to block nonspecific binding. Rabbit anti-human P-Zap70 (1/100; Cell Signaling Technology) was added and incubated for 30 min at room temperature. Cells were rinsed as before in blocking buffer, centrifuged, and resuspended in goat anti-rabbit IgG-PE (1/2000; Southern Biotechnology Associates) in blocking buffer for 30 min at room temperature, rinsed, resuspended in 200 μl of cold PBS, and analyzed by flow cytometry. Isotype and secondary Ab controls were also performed at the same time.

PD-1 and CTLA-4

Cells activated for 3 days with soluble anti-CD3e mAb (145-2C11; 10 μg/ml) were washed with 0.2% BSA/PBS, incubated with rat anti-mouse CD16/32 (2.4G2; 10 μg/ml) to block FcRs, and added hamster anti-mouse CD3e-Alexa 647 (500A2, 4 μg/ml; Invitrogen Life Technologies) and PD-1-PE (RMP1–30; 4 μg/ml), CD4-allophycocyanin (GK1.5), or PD-1-PE (RMP1–30; 4 μg/ml) for 30 min on ice. Appropriate isotype control (hamster IgG-Alexa 647, rat IgG2b-PE, rat IgG2a; 4 μg/ml each) was used. For intracellular T cell CTLA-4 staining, cell surface was stained with hamster anti-CD3-Alexa 647 (500A2, 4 μg/ml; Invitrogen Life Technologies), washed, fixed, and permeabilized for 30 min using the BD Cytofix/Perm kit (BD Biosciences). Cells were then washed using 1× permeabilization buffer, and hamster anti-mouse CTLA-4-PE (UC10-4B9; 4 μg/ml) was added on ice for 30 min. Isotype controls using hamster IgG-Alexa 647 and hamster IgG-PE were also performed accordingly. Cells were washed and suspended in 0.2% BSA/PBS before running the sample on FACSCalibur.

Skin transplantation

Experiments were conducted in B6 mice (recipient) and BALB/c mice (donor) (7–8 wk of age; Charles River Laboratories) and were allowed free access to food and water until the day of surgery. Mice were anesthetized with a regimen that consisted of ketamine (100 mg/kg, i.p.) and xylazine (10 mg/kg, i.p.) and were placed on a thermoregulated pad to maintain body temperature at 37°C. Full-thickness tail skin (1 cm^2) from donor mice was grafted on the dorsal flank area of recipient mice. The skin grafts were secured with paraffin-embedded gauze and with adhesive tape for 5 days. Graft survival was assessed by visual inspection from day 6 to day 9 in a masked fashion. The measured parameters were 1) necrosis, 2) loss of viable tissue, and 3) hair growth. Rejection was diagnosed when the graft loss was ≥70%. At the end of the experimental period, animals were euthanized, and skin graft was removed for H&E staining. Sections were viewed using a Zeiss AxioSkop microscope, and digital images were taken using a SPOT RT Camera (software version 3.3; Diagnostic Instruments). A semiquantitative score was assigned based on the masked reading for thickness of the epidermis (0–2) in which 2 = normal; 1 = loss of <50% thickness; and 0 = loss of >50% thickness and the degree of inflammation (0–5) in which score 0 = normal; 1 = <20%; 2 = 20–40%; 3 = 40–60%; 4 = >60–80%; and 5 = >80% inflammation. Skin allograft recipients were treated with vehicle or ATL313 ($1\ ng \cdot kg^{-1} \cdot min^{-1}$) alone or combined with ZM241385 ($5\ ng \cdot kg^{-1} \cdot min^{-1}$) via osmotic pump (ALZA) ($n = 8$ for each group).

Statistical analysis

Statistical analysis of all dose-response curves was analyzed by two-way ANOVA. Tukey or Bonferroni post hoc analysis was performed to assess significance at specific concentrations in these curves as well as for mean channel fluorescence (MCF) comparisons. Least significant difference post hoc analysis and paired and unpaired Student's *t* tests were also used in some analyses. All curves were fit by nonlinear regression, sigmoidal dose-response parameters. Kaplan-Meier survival curve was used to assess the difference between allograft survival. All statistical analyses were performed using GraphPad Prism version 4.0 (GraphPad). A value of $p < 0.05$ was used to determine significance.

Results

ATL313 attenuates T cell proliferation

In the two-way MLR assay, maximum proliferation of cells was observed by day 3 of culture. Hence, we used this time point to evaluate the effect of various compounds on two-way MLR-induced cell proliferation.

Two-way MLRs were performed in the absence or presence of ATL313 (0.01–100 nM). ATL313 reduced proliferation in a dose-dependent manner with maximum inhibition achieved at a dose of 10 nM (33% of vehicle control, $p < 0.001$, $n = 8$). The addition of the A_{2A}R antagonist ZM241385 (100 nm) attenuated the effect of ATL313 (10 nm; 83% of vehicle control, $p < 0.001$, $n = 6$; Fig. 1*a*).

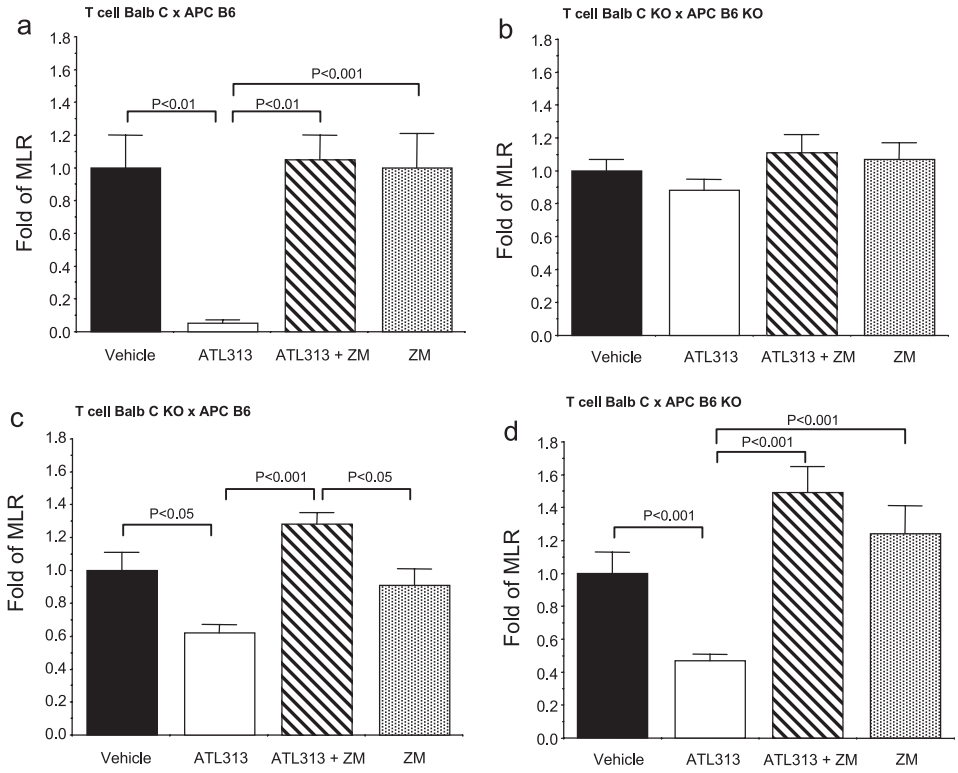

FIGURE 2. ATL313 inhibits lymphocyte proliferation by action on both T lymphocytes and APCs in one-way MLRs. One-way MLRs were performed as described in *Materials and Methods*. Stimulator cells were prepared from spleens of WT (B6 background) or A_{2A}RKO (B6 background) mice and responder spleen T cells were from WT (BALB/c background) or A_{2A}RKO (BALB/c background) mice. We performed four groups of one-way MLR: responder WT × stimulator WT (T cell BALB/c × APC B6) (*a*), responder KO × stimulator KO (T cell BALB/cKO × APC B6 KO) (*b*), responder KO × stimulator WT (T cell BALB/c KO × APC B6) (*c*), and responder WT × stimulator KO (T cell BALB/c × APC B6 KO) (*d*). One-way MLRs were performed in the presence of vehicle, ATL313 (10 nM), ATL313 + ZM241385 (100 nM), and ZM 241385 alone. Experiments were performed in triplicate, $n = 4$ for each group. Values are mean ± SE and are normalized to vehicle group.

The effect of ATL313 was not the result of an increase in apoptosis/necrosis as revealed by annexin V and propidium iodide labeling, markers for apoptosis and necrosis, respectively. There was no significant difference in the level of apoptosis or necrosis when cells were cultured without alloantigen activation (control) or when cells were activated in a two-way MLR. Similarly, the addition of ATL313 and/or ZM241385 did not increase apoptosis/necrosis (data not shown).

To confirm that the attenuation by ATL313 on lymphocyte proliferation was due to activation of A_{2A}Rs, we performed anti-CD3e mAb-induced T cell proliferation by using leukocytes obtained from WT B6 and A_{2A}KO mice (B6 background). In splenocytes obtained from WT B6 mice and stimulated for 24 h with anti-CD3e mAb, ATL313 (0.01–100 nM) reduced lymphocyte proliferation. The effect was maximal at 10 nM (51% of control, $p < 0.001$, $n = 4$). In splenocytes obtained from A_{2A}RKO mice, ATL313 (0.01–100 nM) had no effect (Fig. 1*b*). These results indicate that lymphocyte proliferative responses induced by alloantigens or anti-CD3e mAb are markedly attenuated by specific activation of A_{2A}Rs.

ATL313 inhibits lymphocyte proliferation by action on both T lymphocytes and APCs in one-way MLRs

The ATL313-specific effect on T cell and APC A_{2A}Rs was examined by using A_{2A}R KO mice. In this one-way MLR system, T cells were harvested from BALB/c background WT and/or A_{2A}R KO mice; APCs were harvested from B6 background WT and/or A_{2a}R KO mice. The purity of the negative isolation T cells was >98%. We performed four groups of one-way MLRs: responder WT × stimulator WT (T cell BALB/c × APC B6), responder KO × stimulator KO (T cell BALB/c KO × APC B6 KO), responder KO × stimulator WT (T cell BALB/c KO × APC B6), and responder WT × stimulator KO (T cell BALB/c × APC B6 KO). In one-way MLRs in which both responder and stimulator cells expressed A_{2A}Rs (T cell BALB/c × APC B6), ATL 313 reduced T cell proliferation by 95% ($p < 0.01$; $n = 4$; Fig. 2*a*). This result is consistent with the two-way MLR result observed in Fig. 1*a*. When both responder and stimulator cells lacked A_{2A}Rs (T cell BALB/c KO × APC B6 KO), ATL313 had no significant effect on T cell proliferation (p = NS; $n = 4$; Fig. 2*b*). When

Table I. *Effects of A_{2A}R agonists on two-way MLR-induced cytokine release*[a]

	A (vehicle)	B (ATL)	C (ATL+ZM)	A vs Con	A vs B	B vs C	A vs C
IFN-γ	17.44	3.64	13.84	$p < 0.001$	$p < 0.001$	$p < 0.01$	NS
IL-2	21.87	13.12	21.22	$p < 0.001$	$p < 0.05$	$p < 0.05$	NS
IL-12(p70)	2.15	0.67	1.44	$p < 0.001$	$p < 0.001$	$p < 0.05$	NS
IL-12(p40)	2.14	2.14	1.97	$p < 0.001$	NS	NS	NS
RANTES	2.16	1.44	1.95	$p < 0.001$	$p < 0.001$	$p < 0.001$	NS

[a] Data indicate fold of two-way MLR-induced cytokine and chemokine release over unstimulated control levels. A, vehicle; B, ATL313 (ATL, 10 nm); and C, ATL313 (10 nm) + ZM241385 (ZM, 100 nm). Significance columns assess differences between vehicle and control (A vs Con), vehicle and ATL313 (A vs B), ATL313 and ATL313 + ZM241385 (B vs C), and vehicle and ATL313 + ZM241385 (A vs C), respectively. Values are means, $n = 3$.

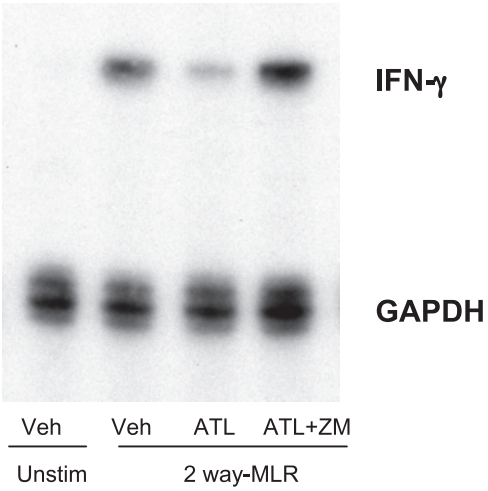

FIGURE 3. Effect of ATL313 on IFN-γ mRNA expression. Total RNA was isolated from cells of two-way MLRs and subjected to RNase protection assay analysis of IFN-γ. A representative photograph of this result is shown. Each lane represents solution hybridization with a radiolabeled probe for IFN-γ and RNA derived from two-way MLRs. GAPDH is shown as a control for loading. Veh, vehicle; unstim, unstimulated; ATL, ATL313; ZM ZM241385.

responder cells (T cell BALB/c KO × APC B6) or stimulator cells (T cell BALB/c × APC B6 KO) lacked A_{2A}Rs, ATL313 reduced T cell proliferation by 38% ($p < 0.05$, $n = 4$; Fig. 2*c*) or 53% ($p < 0.001$, $n = 4$; Fig. 2*d*), respectively. The effect of ATL313 on T cell proliferation was blocked by the A_{2A}R antagonist ZM241385 (Fig. 2, *a*, *c*, and *d*). It is interesting to note that the full effect of ATL313, apparent when both responder and stimulator cells expressed A_{2A}R (Fig. 2*a*), represented an additive effect of

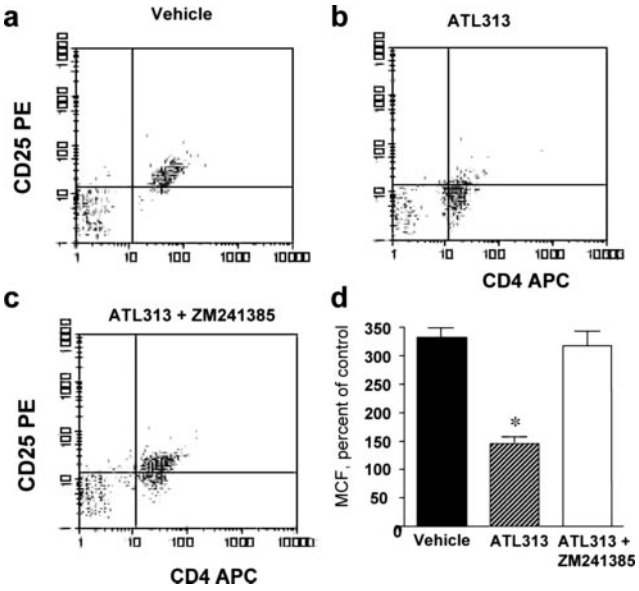

FIGURE 4. Effect of ATL313 on cell surface expression of CD25 on $CD4^+$ T cells in two-way MLRs. *a–c*, Cell surface expression of CD25 (*y*-axis) was measured by gating on $CD4^+$-expressing T cells (*x*-axis) after treatment with vehicle (*a*) or 10 nM ATL313 in the absence (*b*) and presence of 100 nM ZM241385. Levels of CD25 and CD4, as analyzed by flow cytometry, are expressed as MCF of PE and APC, respectively. *d*, Quantitative assessment of CD25 expression. Results represent mean of percentage of control values for unstimulated lymphocytes (100%) ± SEM; $n = 4$; ∗, $p < 0.001$ compared with vehicle or ATL313 + ZM241385.

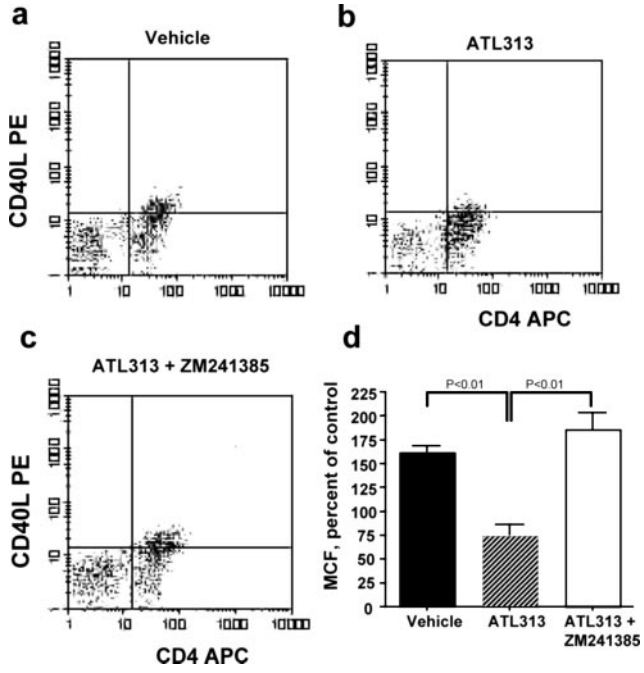

FIGURE 5. Effect of ATL313 on cell surface expression of CD40L on $CD4^+$ T cells in two-way MLRs. *a–c*, Cell surface expression of CD40L (*y*-axis) was measured by gating on $CD4^-$-expressing T cells (*x*-axis) following treatment with vehicle (*a*) or 10 nM ATL313 in the absence (*b*) and presence of 100 nM ZM241385. Levels of CD40L or CD4, as analyzed by flow cytometry, are expressed as MCF of PE and APC, respectively. *d*, Quantitative assessment of CD40L expression. Results represent mean of percentage of control values for unstimulated lymphocytes (100%) ± SEM; $n = 3$.

ATL313 expressed individually on stimulator (Fig. 2*c*) and responder (Fig. 2*d*) cells. These results indicate that A_{2A}Rs expressed on both T cells and APCs mediate the inhibitory effect of lymphocyte proliferation following alloantigen immune activation.

ATL313 inhibits IFN-γ and cytokine release

The effects of ATL313 on two-way MLR-induced cytokine release are summarized in Table I. Using ELISA, the supernatants of two-way MLRs showed a 17-fold increase of IFN-γ over unstimulated lymphocytes that were not mixed in an MLR ($p < 0.001$, $n = 3$). The increase of IFN-γ release was significantly reduced in a dose-dependent manner by ATL313, an effect that was inhibited by the addition of ZM241385 ($p < 0.0001$, $n = 3$). Maximum inhibition of IFN-γ release was observed with 10 nM ATL313 (21% of vehicle, $p < 0.001$, $n = 3$). ZM241385 reduced the response observed with 10 nM ATL-313 to 79% of vehicle (Table I). mRNA from the cultured lymphocytes was harvested at day 3 of culture and analyzed for steady-state IFN-γ mRNA expression by RNase protection assay. Two-way MLRs produced an increase in IFN-γ mRNA expression, an effect that was reduced with 10 nM ATL313. The effect of ATL313 on IFN-γ mRNA expression was blocked by ZM241385 (Fig. 3). Quantitative analysis of band densities, corrected for loading (GAPDH), demonstrated that IFN-γ mRNA increased in MLRs to 10.8-, 5.5-, and 10.5-fold over unstimulated cultured lymphocytes following incubation with vehicle, ATL313, and ATL313 plus ZM241385, respectively ($n = 2$).

Supernatant levels of IL-2, IL-12(p70), IL-12(p40), and RANTES were measured simultaneously by multiplex bead array (Table I). In these studies, cytokines in supernatants obtained from day 3 of two-way MLR cultures were compared with baseline cytokine release from unstimulated cultured lymphocytes. IL-2

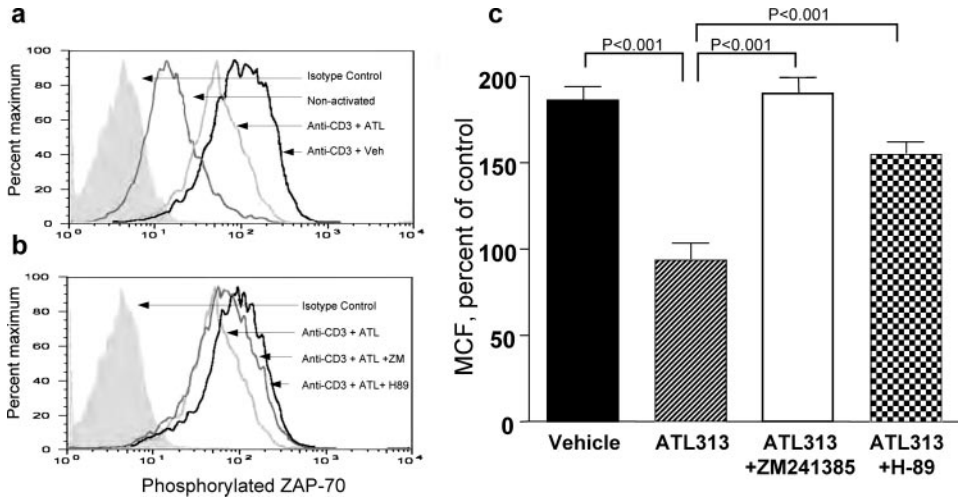

FIGURE 6. Flow cytometric analysis of Zap70 phosphorylation in CD3e mAb-activated lymphocytes. *a*, Histogram overlays depict a rightward shift in levels of phosphorylated Zap70 (as measured by MCF of PE-labeled after activation with CD3e mAb (anti-CD3) under vehicle (veh) treatment compared with nonactivated cells, which is reversed through the addition of 10 nm ATL313 (ATL). *b*, In the same experiment (overlays separated for clarity), the addition of either ZM241385 (ZM; 100 nm) or the protein kinase A inhibitor, H89 (100 nm), to the ATL313-treated group causes a rightward shift of phosphorylated Zap70 compared with ATL313 alone. *c*, Quantitative assessment of the effect of ATL313 on phosphorylated Zap70 is shown. The graph depicts the mean of MCF, expressed as percentage of levels in nonactivated cells (100%), of phosphorylated Zap70 after 5 min of activation with soluble anti-CD3e mAb ± SEM, $n = 3$.

levels in two-way MLRs (69.5 ± 10.0 pg/ml) were 2200% greater than those obtained from supernatants of unstimulated lymphocytes ($p < 0.001$, $n = 3$). ATL313 reduced this alloantigen activated response in a dose-dependent manner with the maximum reduction observed at a concentration of 10 nM ATL313 (60% of vehicle; $p < 0.001$, $n = 3$). This inhibitory effect was completely abrogated by the addition of ZM241385 (98% of vehicle; p = NS, $n = 3$).

IL-12(p70) increased 215% in MLRs (5.7 ± 0.1 pg/ml) when compared with unstimulated lymphocytes ($p < 0.001$, $n = 3$). ATL313 (10 nM) produced a dose-dependent reduction to 31% of vehicle ($p < 0.001$, $n = 3$). The addition of ZM241385 negated the inhibitory effect of ATL313 (67% of vehicle, p = NS, $n = 3$). ATL313 had no inhibitory effect on IL-12(p40) that had increased 214% in the two-way MLR (36.2 ± 1.2 pg/ml). Similarly, the chemokine RANTES, increased by 216% in the two-way MLR (1376.9 ± 82.8 pg/ml) when compared with unstimulated lymphocytes ($p < 0.001$, $n = 3$). ATL-313 (10 nM), reduced this effect to 67% of vehicle ($p < 0.001$, $n = 3$). ZM241385 significantly reversed this effect (90% of vehicle, p = NS, $n = 3$). ATL313 inhibited not only cytokines produced primarily from activated T cells (IFN-γ, IL-2, RANTES) but also from activated DCs (IL-12(p70)).

We also analyzed the effect of ATL313 on a Th2 cytokine profile consisting of IL-6, IL-4, and IL-10. Over the course of 3 days, ELISA showed IL-6 steadily increased in two-way MLRs, but

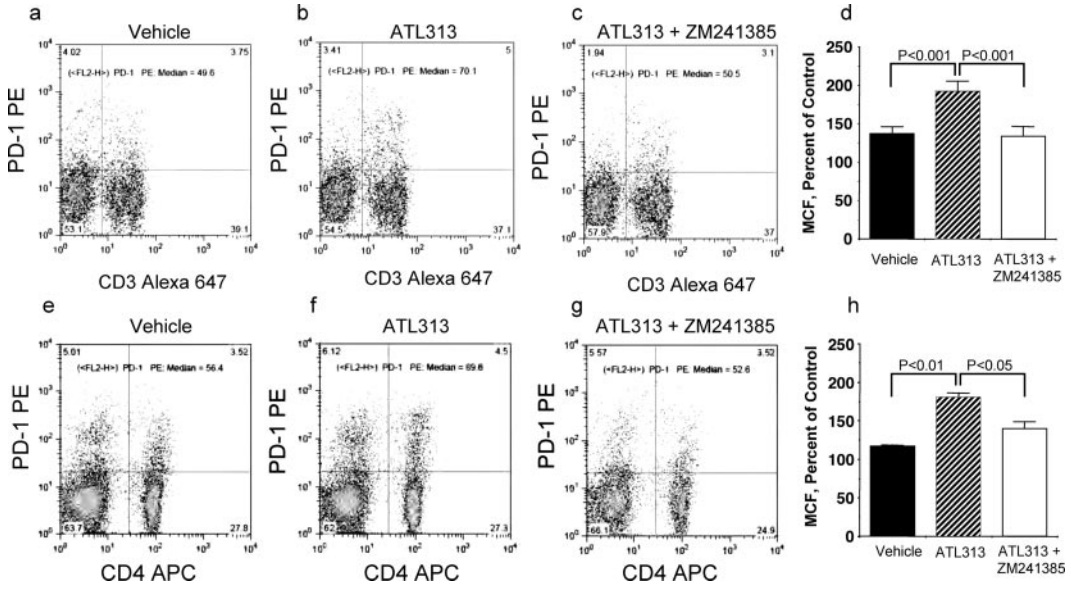

FIGURE 7. Flow cytometric analysis of PD-1 expression on $CD3^+$ and $CD4^+$ cells in two-way MLRs. PD-1 levels in $CD3^+$ (*a–d*)- and $CD4^+$ (*e–h*)-gated events are expressed as MCF of PE. The effect of vehicle (*a* and *e*), ATL313 (10 nM; *b* and *f*), and ATL313 in the presence of ZM241385 (100 nM; *c* and *g*) on the cell surface expression of PD-1 (*y*-axis) and $CD3^+$ (MCF of Alexa 647; $n = 9$) or $CD4^+$ (MCF of APC; $n = 3$) (*x*-axis) is shown. Quantitative assessment of PD-1 expression is shown (*d* and *h*). Results represent mean of control values for unstimulated lymphocytes (100%) ± SEM.

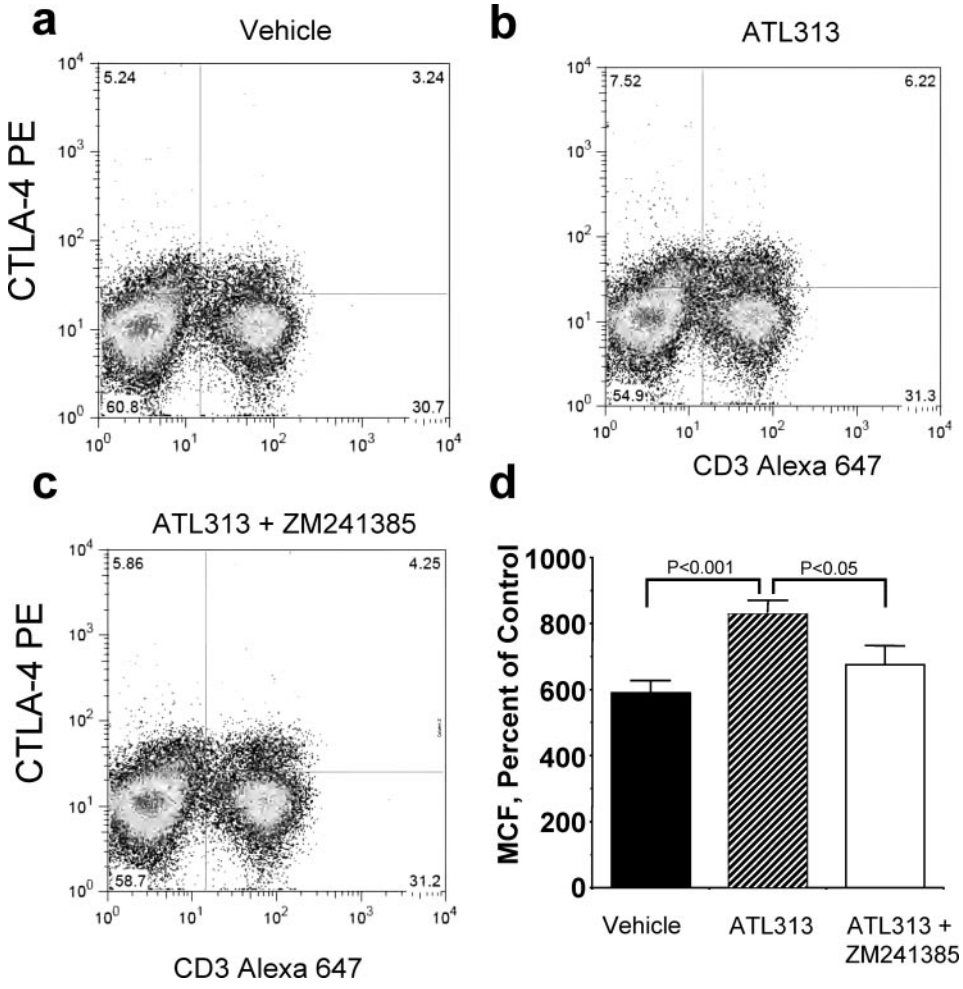

FIGURE 8. Flow cytometric analysis of CTLA-4 expression on $CD3^+$ cells in two-way MLRs. CTLA-4 levels in $CD3^+$-gated events are expressed as MCF of PE. The effect of vehicle (*a*), ATL313 (10 nM; *b*), and ATL313 in the presence of ZM241385 (100 nM; *c*) on the cell surface expression of CLTA-4 (*y*-axis) and $CD3^+$ (MCF of Alexa 647; $n = 8$ (*x*-axis)) is shown. Quantitative assessment (MCF of PE) of CTLA-4 expression is shown (*d*). Results represent mean of control values for unstimulated lymphocytes (100%) ± SEM.

ATL313 did not affect the production of IL-6. IL-4 and IL-10 never reached levels detectable by ELISA over 3 days (data not shown).

ATL313 inhibits expression of CD25 and CD40L on $CD4^+$ T cells activated in two-way MLRs

We next sought to determine the effect of $A_{2A}R$ agonists on the $CD4^+$ T cell activation markers CD25 (the α-chain of the IL-2R; Fig. 4) and CD40L (a costimulatory molecule expressed on active $CD4^+$ cells; Fig. 5). The increase in cell surface expression of CD25 on day 3 of two-way MLR (330 ± 19%, $n = 4$) compared with unstimulated lymphocytes was attenuated with ATL313 (10 nM; 146 ± 12%, $p < 0.001$ compared with vehicle, $n = 4$). ZM241385 (100 nM) reversed this effect of ATL313 on surface expression of CD25 (317 ± 26% of baseline, $p < 0.001$ compared with ATL313, NS compared with vehicle, $n = 4$; Fig. 4).

Similarly, CD40L expression on the cell surface of $CD4^+$ T lymphocytes increased to 161 ± 7% compared with unstimulated cells on day 3 of two-way MLR ($p < 0.01$, $n = 3$), and this increase in CD40L was reduced with ATL313 (10 nM; 74 ± 12% of control, $p < 0.01$ compared with vehicle, $n = 3$). The inhibitory effect of ATL313 was reversed with ZM241385 (186 ± 17% of baseline, $p < 0.01$ compared with ATL313, $p =$ NS compared with vehicle, $n = 3$) (Fig. 5).

ATL313 inhibits anti-CD3e mAb-induced phosphorylation of Zap70

Zap70 is an intracellular tyrosine kinase that is involved in the proximal TCR signaling pathway for the T cell activation. Activation of Zap70 is coupled to downstream signaling cascades, which regulate some critical immune regulatory transcriptional gene. We reasoned that blocking the initial TCR signaling pathway with an $A_{2A}R$ agonist may depress the T cell immune response. Thus, we sought to determine the effect of $A_{2A}R$ activation on Zap70 phosphorylation. After 5 min of T cell activation by soluble anti-CD3e mAb, MCF levels of phosphorylated Zap70 increased by 186 ± 8% when compared with nonactivated cells ($p < 0.001$, $n = 3$), an effect that was reduced to 94 ± 10% of nonactivated cells by ATL313 (10 nM, $p < 0.001$, compared with vehicle $n = 3$). This inhibition of phosphorylated Zap70 by ATL313 was reversed by ZM241385 (100 nM) to 190 ± 10% of nonactivated cells ($p < 0.001$ from ATL313, $p =$ NS from vehicle, $n = 3$). Also, the addition of H-89 (100 nm), a protein kinase A (PKA) inhibitor, blocked the effect of ATL313 by restoring the levels to 155 ± 8% of nonactivated cells ($p < 0.001$ from ATL313, $p =$ NS from vehicle, $n = 3$). One representative example of three experiments can be seen in Fig. 6, *a* and *b*, and a summary of the MCF is illustrated in Fig. 6*c*.

ATL313 induces PD-1 and CTLA-4 expression

We next sought to determine whether ATL313 could up-regulate PD-1 (Fig. 7, *a–d*) and CTLA-4 (Fig. 8) expression, costimulatory molecules that are important in inhibiting T cell activation. As shown in Fig. 7, *a–d*, on day 3 of two-way MLR, the CD3 cell surface expression of PD-1 increased compared with control unstimulated cultured cells (136 ± 10% of control, $n = 9$, $p < 0.001$). The addition of ATL313 further increased T cell PD-1 expression (192 ± 14% of control; $n = 9$; $p < 0.001$ compared

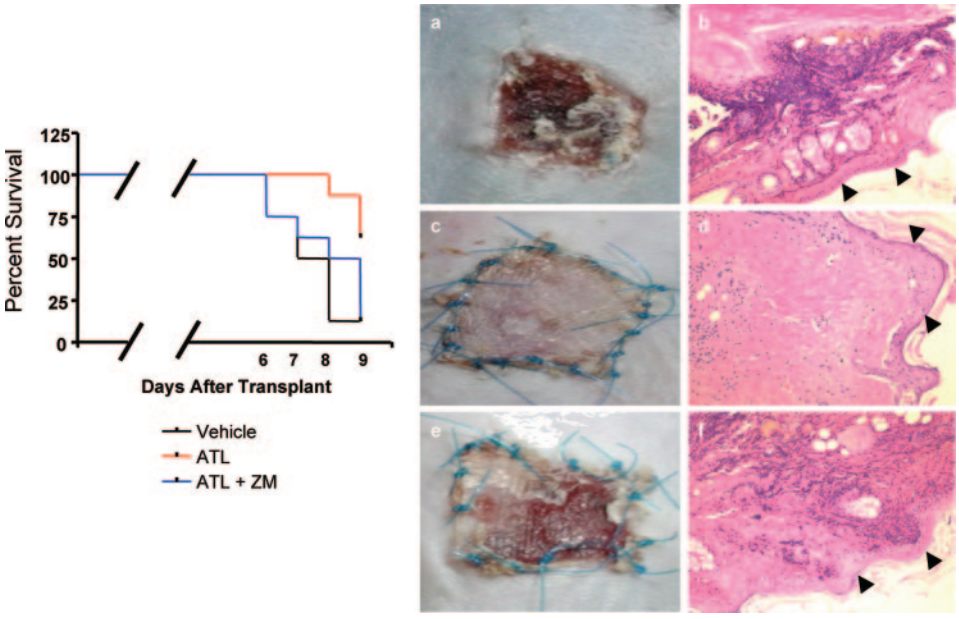

FIGURE 9. ATL313 attenuates skin allograft rejection. Kaplan-Meier curve (*left panel*) for vehicle (black line), ATL313 (red line; ATL; 1 $ng \cdot kg^{-1} \cdot min^{-1}$) and ATL313 + ZM243185 (blue line; ZM; 5 $ng \cdot kg^{-1} \cdot min^{-1}$). $n = 8$ for each group; $p < 0.05$. Photographs (*right panels*) are shown for recipient mice receiving skin allografts. Photographs of transplanted skin (*a*, *c*, and *e*) and H&E sections (*b*, *d*, and *f*) are shown for vehicle (*a* and *b*), ATL313 (*c* and *d*), and ATL313 + ZM241385 (*e* and *f*). Arrowhead, donor epithelium.

with control or vehicle), an effect that was reversed by ZM241385 (134 ± 13% of control, $n = 8$; $p < 0.05$ compared with ATL313; p = NS compared with vehicle). ATL313 also had a similar effect on PD-1 expressed on $CD4^+$ (Fig. 7, *e–h*) and $CD8^+$ T cells (data not shown). Intracellular CTLA-4 expression on activated CD3 cells increased on day 3 of two-way MLR (587 ± 40% of control cells; $n = 7$; $p < 0.001$; Fig. 8). ATL313 induced expression of CLTA-4 in alloantigen-stimulated T cells (820% of unstimulated control cells, $n = 7$, $p < 0.001$ compared with control or vehicle). ZM241385 partially reversed this enhancing effect (681% of control, $n = 7$; $p < 0.001$ compared with control, $p < 0.05$ compared with ATL313).

ATL313 attenuates skin allograft rejection

Our in vitro data provide support that ATL313 inhibits T cell activation, results previously reported (15), and increases negative costimulation. We next tested the hypothesis that ATL313 can block allograft rejection in vivo in a skin transplant mouse model (Fig. 9, Table II). Skin transplants were performed in which full thickness skin grafts from BALB/c donor mice were grafted on the dorsal flank of C57BL/6 mice and treated with vehicle, ATL313 (1 $ng \cdot kg^{-1} \cdot min^{-1}$) alone, or ATL313 combined with ZM241385 (5 $ng \cdot kg^{-1} \cdot min^{-1}$) via osmotic pump ($n = 8$ for each group). Graft survival was assessed by visual inspection from day 6 to day 9 in a masked fashion. As shown by a Kaplan-Meier survival curve (Fig. 9, *left panel*), 9 days after transplantation, the graft survival rate was 12.5, 62.5, and 12.5% for vehicle, ATL313, and ATL313 plus ZM241385, respectively ($n = 8$ for each group; $p < 0.05$). At the end of the experimental period (day 9), skin grafts were harvested and prepared for histology. Photographs of representative skin transplants are shown for vehicle, ATL313, and ATL313 plus ZM241385 (Fig. 9, *a*, *c*, and *e*). There was loss of epidermal skin thickness as well as inflammation in the vehicle group; effects that were reduced with ATL313 treatment. The effects of ATL313 were reversed with ZM241385. Fig. 9, *b*, *d*, and *f*, shows representative H&E staining of the donor skin in vehicle, ATL313, and ATL313 plus ZM241385, and Table II shows semiquantitative scoring of skin thickness and inflammation.

Table II. *Skin transplant histological score with H&E stain*[a]

	Epidermal Thickness	Degree of Inflammation
Vehicle	0.71 ± 0.14	3.71 ± 0.71
ATL313	1.57 ± 0.17**	1.57 ± 0.6*
ATL313 + ZM	0.81 ± 0.13^{++}	3.5 ± 0.60^{+}

[a] Sections were examined at the end of the experimental period (day 9) in a masked fashion under ×400 magnification by light microscopy. The assessment was based on the thickness of the donor epidermis (0–2 score) with 0 = loss of epidermal thickness and 2 = full epidermal thickness, and the degree of inflammation (0–5 score) with 0 = no inflammation and 5 = severe inflammation. Values represent mean ± SEM (*, $p < 0.05$, and **, $p < 0.001$ to vehicle; +, $p < 0.05$, and ++, $p < 0.005$ to ATL313 alone). n = 8/group.

Discussion

The current studies investigated the potential for $A_{2A}R$ agonists to attenuate alloantigen recognition and transplant rejection. We performed MLRs in which splenocytes were isolated from B6 and BALB/c mice and combined in vitro for 3 days with or without ATL313, a selective $A_{2A}R$ agonist. MLR-stimulated T cell proliferation was reduced by ATL313 in a dose-dependant manner with a maximum inhibitory response (~95%) at a dose of 10 nM, an effect reversed by 100 nM of the $A_{2A}R$ antagonist ZM241385. ATL313 attenuated the release from activated T cells and DCs of IFN-γ, RANTES, IL-12(p70), and IL-2 but had no effect on IL-12(p40). ATL313 also inhibited the cell surface expression of T cell activation marker CD25 and CD40L induced by two-way MLRs. In contrast, ATL313 increased surface expression of negative costimulatory molecules PD-1 and CTLA-4 in two-way MLRs. In anti-CD3e mAb-activated lymphocytes, ATL313 still blocked proliferation and inhibited the phosphorylation of Zap70 induced after TCR stimulation, an effect that was reversed by the PKA inhibitor H-89. Lastly, ATL313 attenuated allograft rejection in skin transplants from donor to recipient mice. These results demonstrate that A_{2A} agonists attenuated allogenic recognition by action on T lymphocytes and APCs in vitro, and these effects likely contribute to the attenuation of allograft rejection in vivo. Given our previous observation that $A_{2A}R$ agonists protected kidneys from IRI (12, 14), we believe that $A_{2A}R$ agonists represent a novel class of compounds ideally suited for induction therapy in organ transplantation.

The effect of $A_{2A}R$ agonists to attenuate T cell proliferation in two-way MLRs may be due to effects on $CD4^+$ cells or APCs. To

determine the contribution of A_{2A}Rs expressed on T cells or APCs, we performed one-way MLRs. In one-way MLRs, when A_{2A}Rs were expressed on both responder and stimulator cells, near maximal inhibition of lymphocyte proliferation was achieved. However, when A_{2A}Rs were expressed only on responder or on stimulator cells, only partial inhibition of lymphocyte proliferation was achieved. These results indicate that A_{2A}Rs expressed on both T cells as well as APCs are necessary to maximally inhibit alloantigen recognition.

Clonal expansion of T cells is mediated by the Th1 cytokine IL-2. The production of this cytokine, in conjunction with the α-chain of the IL-2R, CD25, determines whether a naive T cell will become an armed effector T cell and proliferate (21). Lymphocyte proliferation peaked in two-way MLRs at 3 days, and at this same time point, IL-2 levels increased 14-fold in two-way MLR assays over control unstimulated cultured cells. ATL313, when administered to the two-way MLR assays, reduced IL-2 production, CD25 expression, and, subsequently, proliferation. The A_{2A}R antagonist significantly reversed the effects of ATL313 in all instances. These data imply that ATL313 is a potent anti-T cell proliferative agent. ATL313 also inhibits IFN-γ expression, a cytokine that activates macrophages (22), and increases cell surface expression of MHC molecules and Ag-processing components integral to the recognition of foreign Ags (23).

IL-12(p70), the heterodimeric cytokine formed from covalently linked chains of IL-12(p40) and IL-12(p35) (24), is responsible for activation of NK cells and differentiation of $CD4^+$ T cells to Th1-like cells (25). The monomer IL-12(p40) is known to act as an antagonist to the IL-12R (26). Although both IL-12(p70) and IL-12(p40) were increased in two-way MLRs as compared with unstimulated control cells, ATL313 only reduced the active heterodimer, IL-12(p70), and did not affect the monomer IL-12(p40). RANTES, a chemokine released primarily by T cells, is known to activate T cells, is responsible for chronic inflammation, and is a powerful chemoattractant for monocytes, NKT and T cells, basophils, eosinophils, and DCs (27–29). Our results show that ATL313 attenuates secretion of RANTES.

In addition to reducing the release of these cytokines and the expression of CD25, we determined that ATL313 also reduced the cell surface expression of CD40L on $CD4^+$ T cells. CD40L is a costimulatory marker expressed by activated T cells that binds to CD40 on macrophages, working in conjunction with IFN-γ to induce macrophage activation (30, 31). The reduction of both CD40L expression on the cell surface and IFN-γ release from T cells implies that ATL313, in turn, inhibits the activation of monocyte/macrophages. CD40-CD40L is also an important signal pathway for DC and T cell cross-talk, and more important for the initiation of T cells activation, differentiation.

To analyze the mechanisms through which ATL313 mediates $CD4^+$ T cell activation, we stimulated the lymphocytes of a single animal with anti-CD3e mAb to synthetically mimic TCR/CD3 ligation with alloantigens without the dependence on costimulatory markers required by the two-way MLR. In this system, we determined that ATL313 consistently inhibits anti-CD3e mAb-induced proliferation. This suggests that the agonist is able to target the T cell directly and that ATL313 must inhibit a signaling cascade originating with T cells.

Upon binding of TCR/CD3 to its ligand, CD4 and CD45 migrate proximally to the TCR, initiating phosphorylation of the TCR ζ-chain ITAMs by receptor-associated Src-family kinases, such as Fyn. The tyrosine kinase Zap70 binds to the phosphorylated ζ-chain ITAMs and is then phosphorylated by Lck, another Src family kinase bound to the CD4 molecule. Activated Zap70 in turn phosphorylates the linker for activation of T cells and, through a subsequent signaling cascade, activates MAPK-induced phosphorylation events and a wide variety of transcription factors (see Ref. 32 for a review).

To determine the effects of A_{2A}R agonists on the signaling cascade induced by TCR stimulation, we chose to analyze the phosphorylation of Zap70 in $CD4^+$ T cells. We determined by flow cytometric analysis that anti-CD3e mAb activation over a period of 5 min increases levels of phosphorylated Zap70, and the addition of ATL313 significantly reduces those levels. Because the A_{2A}R agonists are believed to increase levels of intracellular cAMP and consequently the activation of PKA (33), we added a PKA inhibitor, H-89, to the assay along with ATL313 and found that levels of phosphorylated Zap70 were restored. These results provide evidence that A_{2A}R agonists inhibit $CD4^+$ T cell activation by inhibiting the phosphorylation of Zap70 through activation of PKA.

Naive T cells are fully activated after receiving signal 1 through TCR-MHC plus antigenic peptide complex and signal 2 through positive costimulatory molecules (34). CD28:B7 signaling is the best characterized and an important costimulatory pathway for naive T cell activation, including cytokine production, clonal expansion, and prevention of anergy and T cell survival (34, 35). However, blocking CD28:B7 pathway wasn't effective in inducing tolerance to murine skin and islet transplantation (36, 37). The negative regulatory signal CTLA-4, which is induced after T cell activation, also can bind both B7-1 and B7-2 molecule and play an important role in down-regulating T cell response in organ transplantation (38, 39). New B7 family ligands PD-L1 and PD-L2 are broadly expressed in nonlymphoid tissues, which are important for regulating the effect of memory T cell responses at the site of inflammation. The finding of accelerated allograft rejection by PD-L1 blockade with Abs confirmed that PD-L1 expression is important for inhibiting the rejection process. We used two-way MLR as an in vitro model to investigate the effect of ATL313 effect on these two negative regulatory costimulatory molecules. We found ATL313 induced PD-1 and CTLA-4 expression on CD3/CD4 T cells. Importantly, T cell activation was not necessary for ATL313 to enhance expression of both PD-1 and CTLA-4. These results suggest that ATL313 inhibits T cell activation, proliferation, and cytokine production by activating the cAMP/PKA pathway to reduce IL-2-induced clonal expansion and to induce the negative regulatory molecules CTLA-4 and PD-1.

These results in vitro suggest potent mechanisms by which A_{2A}R agonists can block alloantigen induced immune responses, responses that mediate transplant rejection. Therefore, we tested whether A_{2A}R agonists can block transplant-mediated tissue rejection. We performed full-thickness skin grafts and found that allograft survival was enhanced following ATL313 administration, an effect reversed by ZM241385. These results provide in vivo evidence that A_{2A}R agonists improved graft survival and can delay transplant rejection.

Our previous studies have shown that A_{2A}R-selective agonists attenuate IRI (12), an effect mediated through $CD4^+$ cells (14). Rag-1 KO mice, deficient in lymphocytes, are protected from IRI, whereas the same animals display the effects of IRI when reconstituted with WT $CD4^+$ T lymphocytes, suggesting that these cells contribute to the initiation of the ischemia-reperfusion-induced inflammatory response. The selective adenosine agonist, ATL146e, a compound that is similar to ATL313 but shorter acting, is unable to inhibit IRI when these mice are reconstituted with A_{2A}R KO $CD4^+$ T lymphocytes (14). These data implicate the $CD4^+$ T lymphocyte as an important target through which A_{2A}Rs inhibit IRI.

In the current study, we found that $A_{2A}R$ agonists attenuate alloantigen recognition through effects mediated by $A_{2A}Rs$ expressed not only on T cells but on APCs as well. Furthermore, $A_{2A}R$ agonists have direct inhibitory effects on $CD4^+$ T cell activation. Thus, these in vitro and in vivo results indicate that $A_{2A}R$ agonists attenuate alloantigen recognition and could induce peripheral T cell tolerance, resulting in improved graft survival. Furthermore, to our knowledge, this is the first demonstration that $A_{2A}R$ agonists delay transplant rejection. The marked efficacy of $A_{2A}R$ agonists in protecting kidneys from IRI in prior studies and allograft rejection in the current studies makes these compounds ideal candidates for induction therapy following organ transplantation.

Acknowledgments

We acknowledge Drs. Timothy Mcdonald (Department of Chemistry, University of Virginia) and Jayson Rieger (Adenosine Therapeutics, Charlottesville, VA) for the gift of ATL313 and Dr. Jiang-Fan Chen (Department of Neurology, Boston University School of Medicine, Boston, MA) for $A_{2A}KO$ mice. We are grateful to Hong Ye and Kailo Schlegel for discussions and technical assistance and Dr. Diane L. Rosin (Department of Pharmacology, University of Virginia) for careful reading of the manuscript and helpful discussions.

Disclosures

M. D. Okusa and J. Linden own equity in Adenosine Therapeutics, which provided ATL313 for this study.

References

1. Sayegh, M. H., and L. A. Turka. 1998. The role of T cell costimulatory activation pathways in transplant rejection. *N. Engl. J. Med.* 338: 1813–1821.
2. Rothstein, D. M., and M. H. Sayegh. 2003. T cell costimulatory pathways in allograft rejection and tolerance. *Immunol. Rev.* 196: 85–108.
3. Greenwald, R. J., Y. E. Latchman, and A. H. Sharpe. 2002. Negative co-receptors on lymphocytes. *Curr. Opin. Immunol.* 14: 391–396.
4. Sho, M., A. D. Salama, A. Yamada, N. Najafian, and M. H. Sayegh. 2001. Physiologic regulation of alloimmune responses in vivo: the role of CTLA4 and Th1/Th2 cytokines. *Transplant. Proc.* 33: 3826–3828.
5. Freeman, G. J., A. J. Long, Y. Iwai, K. Bourque, T. Chernova, H. Nishimura, L. J. Fitz, N. Malenkovich, T. Okazaki, M. C. Byrne, et al. 2000. Engagement of the PD-1 immunoinhibitory receptor by a novel B7 family member leads to negative regulation of lymphocyte activation. *J. Exp. Med.* 192: 1027–1034.
6. Olah, M. E., and G. L. Stiles. 1995. Adenosine receptor subtypes: characterization and therapeutic regulation. *Ann. Rev. Pharmacol. Toxicol.* 35: 581–606.
7. Linden, J. 2001. Molecular approach to adenosine receptors: receptor mediated mechanisms of tissue protection. *Annu. Rev. Pharmacol. Toxicol.* 41: 775–787.
8. Perico, N., D. Cattaneo, M. H. Sayegh, and G. Remuzzi. 2004. Delayed graft function in kidney transplantation. *Lancet* 364: 1814–1827.
9. Reece, T. B., J. D. Davis, D. O. Okonkwo, T. S. Maxey, P. I. Ellman, X. Li, J. Linden, C. G. Tribble, I. L. Kron, and J. A. Kern. 2004. Adenosine A2A analogue reduces long-term neurologic injury after blunt spinal trauma. *J. Surg. Res.* 121: 130–134.
10. Day, Y. J., L. Huang, H. Ye, J. Linden, and M. D. Okusa. 2005. Renal ischemia-reperfusion injury and adenosine 2A receptor-mediated tissue protection: role of macrophages. *Am. J. Physiol.* 288: F722–F731.
11. Glover, D. K., L. M. Riou, M. Ruiz, G. W. Sullivan, J. Linden, J. M. Rieger, T. L. Macdonald, D. D. Watson, and G. A. Beller. 2005. Reduction of infarct size and post-ischemic inflammation from a highly selective adenosine A_{2A} receptor agonist, ATL-146e, in reperfused canine myocardium. *Am. J. Physiol.* 288: H1851–H1858.
12. Okusa, M. D., J. Linden, T. Macdonald, and L. Huang. 1999. Selective A2A-adenosine receptor activation during reperfusion reduces ischemia-reperfusion injury in rat kidney. *Am. J. Physiol.* 277: F404–F412.
13. Day, Y.-J., L. Huang, M. J. McDuffie, D. L. Rosin, H. Ye, J. F. Chen, M. A. Schwarzschild, J. S. Fink, J. Linden, and M. D. Okusa. 2003. Renal protection from ischemia mediated by A_{2A} adenosine receptors on bone marrow-derived cells. *J. Clin. Invest.* 112: 883–891.
14. Day, Y.-J., L. Huang, H. Ye, L. Li, J. Linden, and M. D. Okusa. 2006. Renal ischemia-reperfusion and adenosine 2A receptor-mediated tissue protection: the role of $CD4^+$ T cells and interferon γ. *J. Immunol.* 176: 3108–3114.
15. Lappas, C. M., J. M. Rieger, and J. Linden. 2005. A2A adenosine receptor induction inhibits IFN-γ production in murine $CD4^+$ T cells. *J. Immunol.* 174: 1073–1080.
16. Chen, J. F., Z. Huang, J. Ma, J. Zhu, R. Moratalla, D. Standaert, M. A. Moskowitz, J. S. Fink, and M. A. Schwarzschild. 1999. Nov 1. A_{2A} adenosine receptor deficiency attenuates brain injury induced by transient focal ischemia in mice. *J. Neurosci.* 19: 9192–9200.
17. Copeland, N. G., D. J. Gilbert, N. A. Jenkins, J. H. Nadeau, J. T. Eppig, L. J. Maltais, J. C. Miller, W. F. Dietrich, R. G. Steen, S. E. Lincoln, et al. 1993. Genome maps IV 1993 wall chart. *Science* 262: 67–82.
18. Dietrich, W. F., J. C. Miller, R. G. Steen, M. Merchant, D. Damron, R. Nahf, A. Gross, D. C. Joyce, M. Wessel, R. D. Dredge, et al. 1994. A genetic map of the mouse with 4,006 simple sequence length polymorphisms. *Nat. Genet.* 7: 220–245.
19. Dietrich, W. F., J. Miller, R. Steen, M. A. Merchant, D. Damron-Boles, Z. Husain, R. Dredge, M. J. Daly, K. A. Ingalls, and T. J. O'Connor. 1996. A comprehensive genetic map of the mouse genome. *Nature* 380: 149–152.
20. Potian, J. A., H. Aviv, N. M. Ponzio, J. S. Harrison, and P. Rameshwar. 2003. Veto-like activity of mesenchymal stem cells: functional discrimination between cellular responses to alloantigens and recall antigens. *J. Immunol.* 171: 3426–3434.
21. Cantrell, D. A., and K. A. Smith. 1984. The interleukin-2 T cell system: a new cell growth model. *Science* 224: 1312–1316.
22. Zicari, A., M. Lipari, L. Di Renzo, A. Longo, G. Antonelli, and G. M. Pontieri. 1992. In vivo and in vitro macrophage activation induced by IFN-γ spontaneously released by spleen cells from tumor bearing mice. *J. Biol. Regul. Homeostatic Agents* 6: 65–72.
23. Vegh, Z., P. Wang, F. Vanky, and E. Klein. 1993. Increased expression of MHC class I molecules on human cells after short time IFN-γ treatment. *Mol. Immunol.* 30: 849–854.
24. Gubler, U., A. O. Chua, D. S. Schoenhaut, C. M. Dwyer, W. McComas, R. Motyka, N. Nabavi, A. G. Wolitzky, P. M. Quinn, P. C. Familletti, et al. 1991. Coexpression of two distinct genes is required to generate secreted bioactive cytotoxic lymphocyte maturation factor. *Proc. Natl. Acad. Sci. USA* 88: 4143–4147.
25. Trinchieri, G. 1994. Interleukin-12: a cytokine produced by antigen-presenting cells with immunoregulatory functions in the generation of T-helper cells type 1 and cytotoxic lymphocytes. *Blood* 84: 4008–4027.
26. Germann, T., E. Rude, F. Mattner, and M. K. Gately. 1995. The IL-12 p40 homodimer as a specific antagonist of the IL-12 heterodimer. *Immunol. Today* 16: 500–501.
27. Meurer, R., G. Van Riper, W. Feeney, P. Cunningham, D. Hora, Jr., M. S. Springer, D. E. MacIntyre, and H. Rosen. 1993. Formation of eosinophilic and monocytic intradermal inflammatory sites in the dog by injection of human RANTES but not human monocyte chemoattractant protein 1, human macrophage inflammatory protein 1α, or human interleukin 8. *J. Exp. Med.* 178: 1913–1921.
28. Schall, T. J. 1991. Biology of the RANTES/SIS cytokine family. *Cytokine* 3: 165–183.
29. Schall, T. J., K. Bacon, K. J. Toy, and D. V. Goeddel. 1990. Selective attraction of monocytes and T lymphocytes of the memory phenotype by cytokine RANTES. *Nature* 347: 669–671.
30. Stout, R. D., J. Suttles, J. Xu, I. S. Grewal, and R. A. Flavell. 1996. Impaired T cell-mediated macrophage activation in CD40 ligand-deficient mice. *J. Immunol.* 156: 8–11.
31. Grewal, I. S., and R. A. Flavell. 1996. A central role of CD40 ligand in the regulation of $CD4^+$ T cell responses. *Immunol. Today* 17: 410–414.
32. Qian, D., and A. Weiss. 1997. T cell antigen receptor signal transduction. *Curr. Opin. Cell Biol.* 9: 205–212.
33. Skalhegg, B. S., and K. Tasken. 2000. Specificity in the cAMP/PKA signaling pathway: differential expression, regulation, and subcellular localization of subunits of PKA. *Front. Biosci.* 5: D678–D693.
34. Linsley, P. S., and J. A. Ledbetter. 1993. The role of the CD28 receptor during T cell responses to antigen. *Annu. Rev. Immunol.* 11: 191–212.
35. Dahl, A. M., C. Klein, P. G. Andres, C. A. London, M. P. Lodge, R. C. Mulligan, and A. K. Abbas. 2000. Expression of bcl-X_L restores cell survival, but not proliferation off effector differentiation, in CD28-deficient T lymphocytes. *J. Exp. Med.* 191: 2031–2038.
36. Larsen, C. P., E. T. Elwood, D. Z. Alexander, S. C. Ritchie, R. Hendrix, C. Tucker-Burden, H. R. Cho, A. Aruffo, D. Hollenbaugh, P. S. Linsley, et al. 1996. Long-term acceptance of skin and cardiac allografts after blocking CD40 and CD28 pathways. *Nature* 381: 434–438.
37. Trambley, J., A. W. Bingaman, A. Lin, E. T. Elwood, S. Y. Waitze, J. Ha, M. M. Durham, M. Corbascio, S. R. Cowan, T. C. Pearson, and C. P. Larsen. 1999. Asialo $GM1^+CD8^+$ T cells play a critical role in costimulation blockade-resistant allograft rejection. *J. Clin. Invest.* 104: 1715–1722.
38. Ansari, M. J., A. D. Salama, T. Chitnis, R. N. Smith, H. Yagita, H. Akiba, T. Yamazaki, M. Azuma, H. Iwai, S. J. Khoury, et al. 2003. The programmed death-1 (PD-1) pathway regulates autoimmune diabetes in nonobese diabetic (NOD) mice. *J. Exp. Med.* 198: 63–69.
39. Salama, A. D., T. Chitnis, J. Imitola, M. J. Ansari, H. Akiba, F. Tushima, M. Azuma, H. Yagita, M. H. Sayegh, and S. J. Khoury. 2003. Critical role of the programmed death-1 (PD-1) pathway in regulation of experimental autoimmune encephalomyelitis. *J. Exp. Med.* 198: 71–78.